



Enhanced SOFC Cathode Performance Through Surface Modification of $\text{NdBa}_{0.5}\text{Sr}_{0.5}\text{Co}_2\text{O}_{5+\delta}$ Nanoparticles

Adi Subardi

Department of Mechanical Engineering, Institut Teknologi Nasional Yogyakarta, Daerah Istimewa Yogyakarta 55281, Indonesia

Corresponding author: subardi@sttnas.ac.id

<https://doi.org/10.14710/jksa.25.9.322-328>



Article Info

Article history:

Received: 7th August 2022

Revised: 28th November 2022

Accepted: 29th November 2022

Online: 23rd December 2022

Keywords:

SOFC; Cathode; Electrical conductivity; Infiltration; Long-term performance stability

Abstract

The cathode materials fabrication with outstanding performance and stability at intermediate temperatures of 600–800°C is required for the prospective mass production of solid oxide fuel cells (SOFCs). Infiltration is a potential method because it has proven successful in fabrication and cell performance enhancement. This study mainly focuses on the electrical conductivity and long-term reliability of cathode symmetric cells $\text{NdBa}_{0.5}\text{Sr}_{0.5}\text{Co}_2\text{O}_{5+\delta}$ (NBSC) fabricated by traditional solid-state reaction techniques. The electrical conductivity value of the cathode is in the range of 174–278 $\text{S}\cdot\text{cm}^{-1}$. Impedance analysis showed that the infiltration of 0.5M SDC on the NBSC cathode surface dramatically reduced the polarization resistance (R_p) between layers (cathode–electrolyte) from 3.32 $\Omega\cdot\text{cm}^2$ to 1.82 $\Omega\cdot\text{cm}^2$ at 600°C or decreased by 45 % compared to NBSC cathode without 0.5M SDC infiltration. The enhanced stability of NBSC cathode specimens with 0.5M SDC infiltration (NBSC+0.5 M SDC) under SOFC operating conditions proves that samples with infiltration extend their lifetime. Compared to the NBSC cathode, the NBSC+0.5 M SDC cathode has better long-term stability with a lower R_p value of 2.35 $\Omega\cdot\text{cm}^2$. In the OPP range of 0.214–0.0027 atm at 800°C, the relatively tiny R_p value of the symmetrical cell is between 0.030 $\Omega\cdot\text{cm}^2$ and 0.039 $\Omega\cdot\text{cm}^2$, below the 0.15 $\Omega\cdot\text{cm}^2$ suitable performance limit for solid oxide fuel cells.

1. Introduction

Although plenty of fossil fuels are still available, critical technological advancements have been made, and the demand for ecological and environmental preservation is increasing [1]. Fuel cells (FC) and hybrid electric vehicles play a significant role in decreasing carbon dioxide pollution. By using the H_2 generated by this process, FC vehicles (FCVs) can reduce CO_2 emissions in this sector to 80% compared to traditional vehicles [2]. In a global effort to overcome the dangers of climate change, cogeneration systems, especially fuel cells, are becoming massive due to their excellent energy efficiency [3].

Solid oxide fuel cells (SOFCs) are the most environmentally friendly electrical energy generator and effective electrochemical energy converter. The current weakness of SOFCs is the high operating temperature of

800–1000°C, which significantly affects cost, reliability, and application. The focus of SOFC development is efforts to reduce the working temperature of SOFC between 600 to 800°C. Unfortunately, the low working temperature causes the SOFC electrode kinetics to decrease. Two essential strategies can be used to develop SOFCs today, namely (a) reducing ohmic resistance; (b) reducing the polarization resistance of the cathode [4, 5]. Cathode development continues to be carried out to improve electrode and cathode optimization as a factor that determines the overall SOFC performance [6].

Materials that provide ionic and electronic conduction (mixed ionic–electronic conductors, MIEC) can minimize polarization resistance [7]. Most oxide compositions with a perovskite structure show mixed conductivity in the medium temperature range [8]. Cobalt-containing double perovskite-based cathodes exhibited excellent electrochemical activity and

compatibility with SDC doping electrolytes [9, 10]. Cobalt-based mixed ionic–electronic conductors such as $\text{LnBa}_{0.5}\text{Sr}_{0.5}\text{Co}_{1.5}\text{Fe}_{0.5}\text{O}_{5+\delta}$ [11], $\text{Pr}_{0.5}\text{Y}_{0.5}\text{BaCo}_2\text{O}_{5+\delta}$ [12], $\text{SmBaCo}_{2-x}\text{Ni}_x\text{O}_{5+\delta}$ [13], $\text{PrBaCo}_{2-x}\text{Mn}_x\text{O}_{5+\delta}$, [14], $\text{NdBa}_{0.25}\text{Sr}_{0.75}\text{CoCuO}_{5+\delta}$, [15], $\text{YBa}_{0.5}\text{Sr}_{0.5}\text{Co}_{2-x}\text{Fe}_x\text{O}_{5+\delta}$, [16], $\text{SmBa}_{1-x}\text{Sr}_x\text{Co}_2\text{O}_{5+\delta}$ [17], $\text{GdBa}_{0.5}\text{Sr}_{0.5}\text{Co}_{1.5}\text{Fe}_{0.5}\text{O}_{5+\delta}$ [18], $\text{YBa}_{0.7}\text{Sr}_{0.3}\text{Co}_2\text{O}_{5+\delta}$ [19], and $\text{YBaCo}_2\text{O}_{5+\delta}$ [20] have been published as promising materials for IT–SOFC cathodes. The coefficient of thermal expansion (TEC) of SOFC components (cathode, electrolyte anode, and interconnection material) must be similar in order to obtain efficient operation.

One effective method to reduce the thermal expansion coefficient (TEC) and improve electrochemical performance is through the infiltration/impregnation method of electrolyte material into a porous cathode to obtain a composite cathode. Using composite cathodes in SOFC devices reduces TEC and expands the cathode layer’s three-phase boundary zone (TPB) [21]. In this work, catalytically active $\text{Ce}_{0.8}\text{Sm}_{0.2}\text{O}_{1.9}$ (SDC) nanoparticles were infiltrated into the NBSC cathode to improve the catalytic activity of the SDC electrolyte-based electrode. The cathode properties of the NBSC were evaluated for electrical conductivity and electrochemical impedance spectroscopy during long-term performance testing. Novelty in this article is the cathode design using double perovskite oxide doped with 0.5 M electrolyte material. This work suggested that a double perovskite-based cathode material is appropriate for IT–SOFC applications.

2. Experimental

2.1. Preparation of cathode materials and electrolytes

The $\text{NdBa}_{0.5}\text{Sr}_{0.5}\text{Co}_2\text{O}_{5+\delta}$ (NBSC) cathode was fabricated using the solid-state reaction method. The precursors use high-grade materials Nd_2O_3 , SrCO_3 , BaCO_3 , and CoO . The milled material was dried, crushed into a powder using a grinder, and then calcined for four hours at 1100°C in the air. The $\text{Ce}(\text{NO}_3)_3 \cdot 6\text{H}_2\text{O}$ and $\text{Sm}(\text{NO}_3)_3 \cdot 6\text{H}_2\text{O}$ were used to synthesize the electrolyte powder SDC as a precursor material. The precursor material was dissolved in distilled water, then added to the ammonia solution with this stoichiometric ratio. After the mixture’s pH was adjusted to 9.5 to 10, coprecipitation powder was heated for two hours at 600°C in the air. The reference [22] provides detailed instructions for SDC fabrication.

Table 1. Composition and abbreviation of $\text{NdBa}_{0.5}\text{Sr}_{0.5}\text{Co}_2\text{O}_{5+\delta}$ based specimens

Composition	Abbreviation
$\text{NdBa}_{0.5}\text{Sr}_{0.5}\text{Co}_2\text{O}_{5+\delta}$	NBSC
$\text{NdBa}_{0.5}\text{Sr}_{0.5}\text{Co}_2\text{O}_{5+\delta} + 0.5 \text{ M SDC}$	NBSC+0.5 M SDC

The infiltration technique procedures are detailed in reference [23, 24]. For fabrication of the required SDC nanoparticles in the NBSC porous cathode, symmetric cells impregnated with 0.5M SDC, hereinafter abbreviated as NBSC+0.5M SDC, were heated at 900°C for 2 hours. The $\text{Ce}(\text{NO}_3)_3 \cdot 6\text{H}_2\text{O}$ and $\text{Sm}(\text{NO}_3)_3 \cdot 6\text{H}_2\text{O}$ were dissolved in deionized water to create an aqueous nitrate solution of the $\text{Ce}_{0.8}\text{Sm}_{0.2}(\text{NO}_3)_3$ precursor. The porous cathode was

coated on either side with 0.5M SDC nanoparticle liquid using the microliter injector.

2.2. Specimen testing

The NBSC pellets measuring $5 \times 5 \times 10 \text{ mm}^3$ were sintered at 1200°C for an hour and were used as electrical conductivity test specimens. Electrical conductivity was investigated by the four-probe DC method, and the voltage response was recorded using a Keithley 2420 Source Meter at a temperature between 300°C and 800°C by applying a continuous current to the two current wires. For electrochemical testing of symmetrical cell samples, the NBSC-based cathode was utilized as the working electrode (WE). The Ag counter electrode (CE) was placed on the opposite side of the sintered SDC disk, and the reference electrode (RE) was fabricated 3–4 mm from the WE. Screen-printing was used to coat the NBSC-based cathodes on both sides of the SDC electrolyte, and they were further sintered in the air at 1000°C for four hours.

Cell stability testing was carried out for 96 hours without stopping at 600°C . The symmetric cell test was also performed under various atmospheric pressure $P(\text{O}_2) = 0.112 \text{ atm} - 0.019 \text{ atm}$ at a temperature between 600°C and 800°C . The applied frequency ranges from 100 kHz to 0.1 Hz with an AC amplitude signal of 10 mV. The AC impedance measurement calculated the current density value (i_o). The formula (1) adapted from the Butler–Volmer formula was used to calculate the value of i_o , and the total cathode R_p was calculated from the intersection with the axis of the impedance loop [25].

$$i_o = \frac{RTv}{nFR_p} \tag{1}$$

where, F is Faraday’s factor ($F = 96,500 \text{ C mol}^{-1}$), R is the ideal gas constant ($R = 8.31 \text{ J mol}^{-1}\text{K}^{-1}$), the total electrons number transferred in the reaction is given by the notation n , and the number of times the rate-determining step begins in a whole reaction event is given by the notation v . For oxygen reduction reactions, n and v are commonly used to be 4 and 1, respectively. The comprehensive calculating process refers to reference [26].

3. Results and Discussion

3.1. NBSC cathode electrical conductivity

Figure 1 shows the relationship between temperature and the NBSC cathode electrical conductivity at $P(\text{O}_2) = 0.03 \text{ atm}$ and 0.0032 atm at 300 to 800°C . It can be seen that at $P(\text{O}_2) = 0.03 \text{ atm}$ (red line), at a temperature of 302°C it has reached the highest electrical conductivity value of 278 S.cm^{-1} . Defects in the Co–O–Co bond lattice cause the release of oxygen atoms from the lattice and the reduction of Co^{4+} to Co^{3+} or Co^{3+} to Co^{2+} to cause a significant drop in electrical conductivity beginning at 330°C . At 440°C the rate of decrease in conductivity slows down and forms a linear line from 552 to 800°C . At $P(\text{O}_2) = 0.0032$ (blue line), the reduction in electrical conductivity starts from the initial heating of 300°C to 603°C , forming a linear line.

Conductivity began moving slowly at $611-663^\circ\text{C}$, increasing significantly to 800°C . NBSC cathode

conductivity values are 174–278 S.cm⁻¹ and meet the requirements of SOFC cathode material [27]. The metallic conductivity properties of NBSCs can be related to several factors [19, 28, 29]: (1) energy bands overlap between Co- 3d and O-2p; (2) the presence of Co⁴⁺ ions from the thermally affected Co³⁺ charge disproportion; and (3) loss of oxygen from the lattice at higher temperatures.

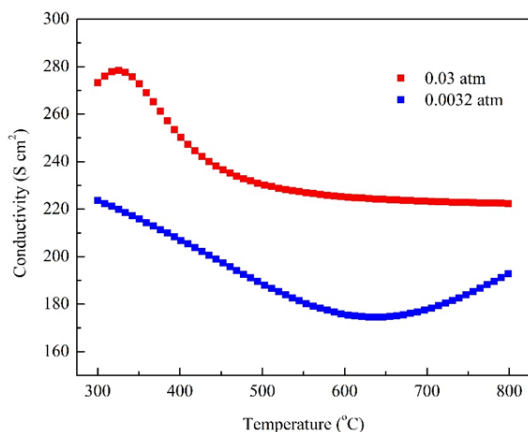


Figure 1. NBSC cathode conductivity at P(O₂) = 0.03 atm and P(O₂) = 0.0032 atm to temperature

Cobalt-containing perovskites are widely investigated because of their high electronic and oxide-ionic conductivity values. The conductivity value of this material exceeds perovskite oxide with other 3d transition metal ions [30]. Measurement of the NBSC cathode shows a relatively high electrical conductivity value above 100 S.cm⁻¹, indicating that it is a p-type electronic conductor. The total value of the conductivity of the NBSC sample is a combination of the electronic ions' conductivity and oxides caused by the existence of electron-hole pairs and oxygen vacancies. The ionic conductivity of the perovskite-type oxide material is

significantly lower than the electronic conductivity. Therefore, it can be concluded that electronic conductivity dominates the conductivity value [31]. As previously reported that the activation energy (E_a) of the NBSC cathode polarization resistance from the Ln(R) vs. 1000/T is 102.5 kJ mol⁻¹ [32].

3.2. Symmetrical cell long-term test

The specimens were evaluated using AC impedance spectroscopy under an open circuit. The symmetrical cell performance was examined to assess the NBSC long-term stability, and the polarization resistance (R_p) value was measured versus time in stationary air at 600°C. Figure 2(a)-(e) shows NBSC cathodes with and without SDC infiltration and the R_p value as a function of time under stationary air as an oxidant in the 2 to 96 hours. The R_p value of the NBSC+0.5 M SDC cathode decreased significantly from 3.32 Ω.cm² to 1.82 Ω.cm² or decreased by 45% compared to the NBSC cathode without infiltration.

The R_p value of NBSC+0.5 M SDC cathode in this study is still better than that achieved by cathodes GdBa_{0.5}Sr_{0.5}Co_{1.5}Fe_{0.5}O_{5+δ} [18] and YBa_{0.7}Sr_{0.3}Co₂O_{5+δ} [19], which are 2.33 Ω.cm², and 3.29 Ω.cm², respectively. The R_p value decline was primarily due to the additional SDC|NBSC+0.5 M SDC phase limit. Gas-phase molecules can easily migrate into the SDC|NBSC+0.5 M SDC interlayer, mainly to the produced nano-sized SDC particles on the very porous NBSC surface cathode. The oxygen reduction reaction (ORR) activity in electrochemical sites significantly increases under these conditions. The ORR is on the surface area of the NBSC cathode, simultaneously hitting the electrolyte and air. These newly formed SDC nanoparticles were deposited on the NBSC porous framework [24].

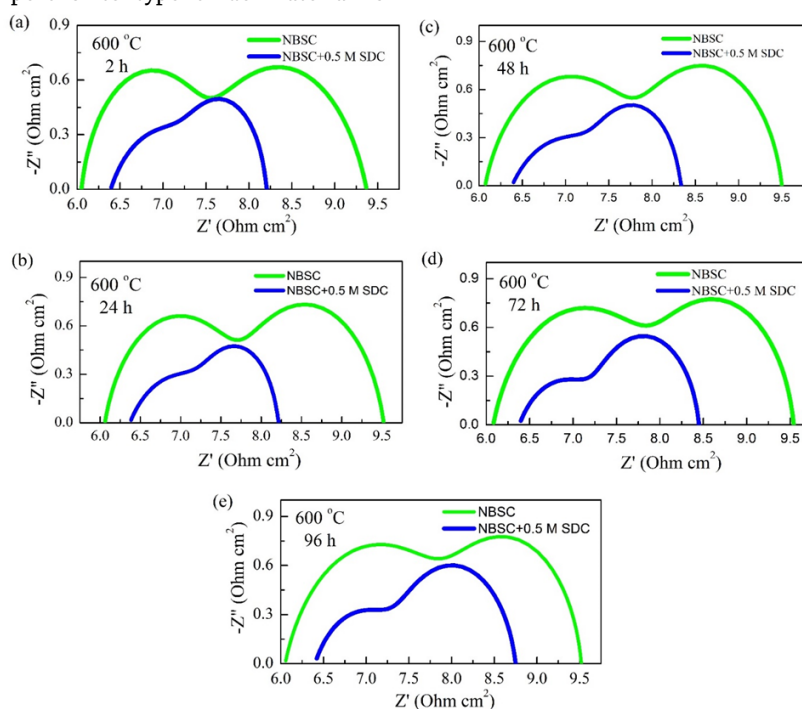


Figure 2. Long-term test: (a) Nyquist diagram of symmetrical cell spectroscopic impedance NBSC|SDC|NBSC and (b) NBSC+0.5 M SDC |SDC|NBSC+0.5 M SDC in the temperature range 2–96 hours at 600°C

The R_p value of the NBSC+0.5 M SDC cathode specimen increases gradually over time, whose value goes up from $1.82 \Omega \cdot \text{cm}^2$ in the initial 2 hours to $2.35 \Omega \cdot \text{cm}^2$ on a long-term test of 96 hours at 600°C as shown in Table 2. A slight improvement in the cathodic R_p , and the rising rate was about $0.55\% \text{ h}^{-1}$ from the initial 2 to 96 hours. The NBSC+0.5 M SDC cathode sample has better long-term stability than NBSC, with a lower R_p value of $2.35 \Omega \cdot \text{cm}^2$. Figure 3 shows the polarization resistance rate between the NBSC cathode and NBSC+0.5 M SDC.

Table 2. R_p Value of symmetrical cells for NBSC and NBSC+0.5 measured during 96 hours at 600°C

Time (hours)	$R_p (\Omega \cdot \text{cm}^2)$	
	NBSC	NBSC+0.5 M SDC
2	3.32	1.82
12	3.39	1.86
24	3.46	1.85
36	3.40	1.92
48	3.43	1.96
60	3.40	2.05
72	3.46	2.07
84	3.43	2.26
96	3.47	2.35

The cathode delamination of the electrolyte can be one of the possible causes of the increased R_p at the beginning of rapid degradation. Delamination between layers affects a drop in the activity site of the ORR, which causes an improvement in polarization resistance. According to previous studies, the difference between NBSC ($\text{TEC} = 25.2 \text{ ppm K}^{-1}$) and SDC ($\text{TEC} = 12.4 \text{ ppm K}^{-1}$) is approximately 12.8 ppm K^{-1} [22]. After testing, the surface of the cathode sample experienced agglomeration. The microstructure growth, such as grain

expansion or particle coarsening, is critical since a practical SOFC operates at high temperatures (at $T = 800\text{--}1000^\circ\text{C}$) [33]. With increasing temperature and current density, as well as the duration of the test, the microstructure gets coarser and denser [34].

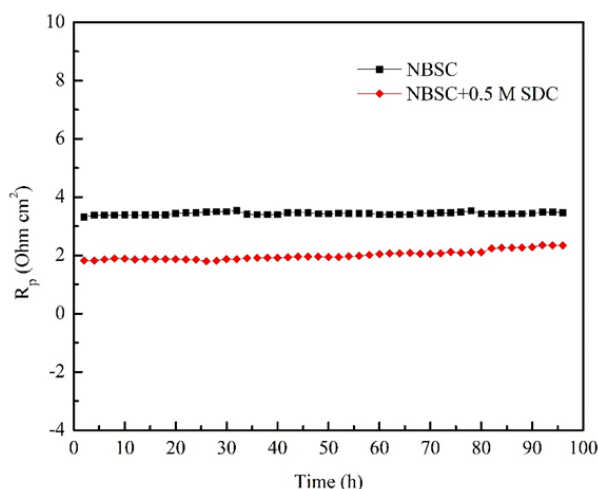


Figure 3. Polarization resistance (R_p) curve for long-term symmetric cell testing: (a) NBSC|SDC|NBSC, and (b) NBSC+0.5 M SDC|SDC|NBSC+0.5 M SDC

3.3. Symmetric cell measurement in various OPP

To further investigate the oxygen reduction reaction process of the symmetrical specimen NBSC+0.5 M SDC|SDC|NBSC+0.5 M SDC. The electrochemical impedance spectroscopy (EIS) was tested at different partial pressures of oxygen (OPP) according to previously published papers [22]. The R_p values are based on the Nyquist diagram of NBSC+0.5 M SDC cathode impedance spectroscopy on SDC electrolytes with various OPP at various temperatures, as shown in Figure 4.

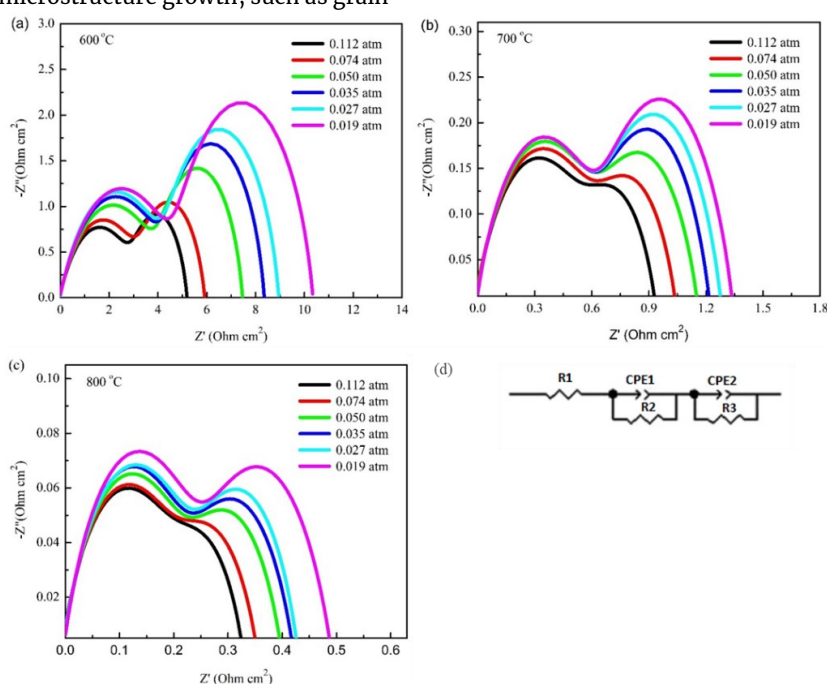


Figure 4. (a)–(c) Nyquist diagram of impedance spectroscopic symmetric cell NBSC+0.5 M SDC|SDC|NBSC+0.5 M SDC in the OPP range between 0.112–0.019 atm at various temperatures and (d) Equivalent circuit used to fit the impedance spectra

The polarization resistance values increase with decreasing OPP at 600, 700, and 800°C, respectively. At a temperature of 600°C, the value of the polarization resistance (R_p) increases from 3.69 $\Omega\cdot\text{cm}^2$ (0.112 atm) to 6.05 $\Omega\cdot\text{cm}^2$ (0.019 atm). At 700°C, the pattern is the same; the R_p value increases from 0.75 $\Omega\cdot\text{cm}^2$ to 1.17 $\Omega\cdot\text{cm}^2$ at 0.112 atm and 0.019 atm, respectively. Also, at 800°C, the polarization resistance increases from 0.030 $\Omega\cdot\text{cm}^2$ to 0.039 $\Omega\cdot\text{cm}^2$ at OPP = 0.112 atm and 0.019 atm, respectively.

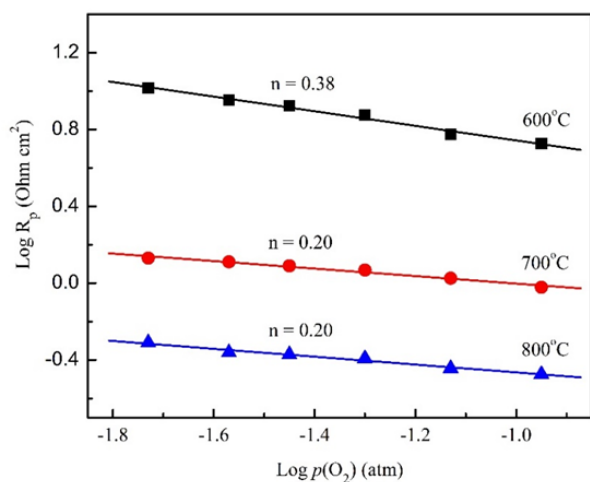


Figure 5. Polarization resistance between layers as a function of oxygen partial pressure (OPP) symmetrical cell NBSC+0.5 M SDC|SDC|NBSC+0.5 M SDC at various temperatures

The resistance of the evaluation cell was demonstrated using an analogous circuit of the impedance curve and was fitted using Z-View based on the following series circuit $R_1 (R_2-CPE_1) R_3-CPE_2$. The R is the same as Ohmic resistance ($R\Omega$), and polarization resistance is characterized by two resistances (R_2+R_3). A constant phase element (CPE) symbolizes a non-ideal capacitor, such as the double layer at a nonplanar TPB. The n parameter correlated with the CPE equivalent to a real capacitor, where $n=1$.

The $\log (R_p)$ as a function of $\log P(O_2)$ cathode NBSC+0.5 M SDC measured at various temperatures is

illustrated in Figure 5. It is evident that as $P(O_2)$ decreases, the value of R_p rises due to a reduction in mobile interstitial oxygen at lower $P(O_2)$. The R_p value of symmetrical cells in the OPP range of 0.214–0.0027 atm at various temperatures, as shown in Table 3. The value ranges between $n = 0.20$ and $n = 0.38$, depending on the slope of the curve. The result shows that the primary ORR process is dominated by the charge transfer process (charge transfer processes) TPB and/or site 2PB cathode NBSC+0.5 to the electrolyte in the temperature range 600–800°C [35]. The transfer of electrons and oxygen is closely related to the cathode structure, which impacts fuel cell performance, including reaction kinetics and charge and mass transfer preprocessing.

Table 3. The R_p value of symmetrical cells in the OPP range of 0.214–0.0027 atm at various temperatures

OPP (atm)	600°C	700°C	800°C
	$R_p (\Omega\cdot\text{cm}^2)$	$R_p (\Omega\cdot\text{cm}^2)$	$R_p (\Omega\cdot\text{cm}^2)$
0.112	3.69	0.75	0.030
0.074	3.99	0.82	0.032
0.050	4.54	0.91	0.033
0.035	5.06	1.02	0.035
0.027	5.61	1.08	0.038
0.019	6.05	1.17	0.039

The microstructure of the NBSC+0.5 M SDC cathode surface and the cross-sectional microstructure of the two layers (cathode and electrolyte) are presented in Figure 6. The adhesion of the two layers (cathode and electrolyte) looks strong. The grain size was evenly distributed in the range of 1–2 μm , and the microstructure of the NBSC+0.5 M SDC cathode was porous. A good SOFC cell morphology includes (1) a porous cathode microstructure, (2) interlayer (electrolyte–cathode) connectivity, and (3) a dense electrolyte layer. Good morphology promotes rapid oxygen diffusion, minimizes polarization resistance, and improves current collection. The surface morphology of the NBSC+0.5 M SDC sample corresponds to the physical characteristics of the SOFC cathode. The limit for reasonable performance solid oxide fuel cell (SOFC) value is $R_p < 0.15 \Omega\cdot\text{cm}^2$. The surface morphology of the NBSC+0.5 M SDC sample corresponds to the physical characteristics of the SOFC cathode.

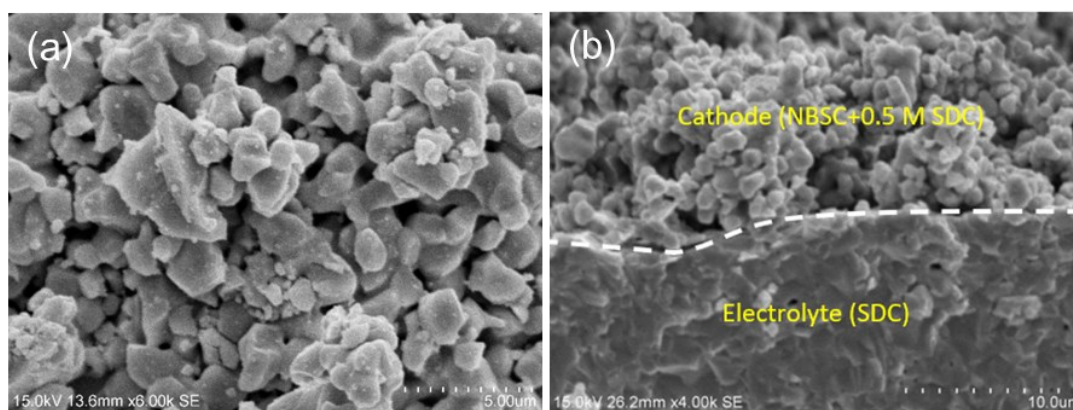


Figure 6. SEM images (a) The cathode surface and (b) the cross-sectional microstructure of the two layers (cathode and electrolyte)

4. Conclusion

This research analyzes the electrical conductivity, infiltration impact, and stability of the cathode operating at an intermediate temperature of 600–800°C. The NBSC cathode conductivity values are in the range that meets the requirements of SOFC cathode materials. The surface morphology of the NBSC+0.5 M SDC sample matches the physical properties of the SOFC cathode. The relatively small Rp value of the symmetrical cell is between 0.030 Ω.cm² and 0.039 Ω.cm² in the OPP range 0.214–0.0027 atm at 800°C, below 0.15 Ω.cm² the reasonable performance limit for solid oxide fuel cells (SOFC). The infiltration of 0.5 M SDC on the NBSC porous cathode significantly reduced the interlayer's polarization resistance value by almost half compared to that of the NBSC cathode without 0.5 M SDC infiltration. The NBSC+0.5 M SDC cathode specimen demonstrated stability under SOFC operating conditions and increased operational life compared to non-infiltrated cathodes.

Acknowledgment

Thank you to Prof. Yen-Pei Fu from the MSE Department at NDHU Taiwan, who provided lab facilities and in-depth discussions.

References

- [1] Caineng Zou, Qun Zhao, Guosheng Zhang, Bo Xiong, Energy revolution: From a fossil energy era to a new energy era, *Natural Gas Industry B*, 3, 1, (2016), 1-11 <https://doi.org/10.1016/j.ngib.2016.02.001>
- [2] Jung-Ho Wee, Contribution of fuel cell systems to CO₂ emission reduction in their application fields, *Renewable and Sustainable Energy Reviews*, 14, 2, (2010), 735-744 <https://doi.org/10.1016/j.rser.2009.10.013>
- [3] Kazui Yoshida, Hom B. Rijal, Kazuaki Bohgaki, Ayako Mikami, Hiroto Abe, Energy-saving and CO₂-emissions-reduction potential of a fuel cell cogeneration system for condominiums based on a field survey, *Energies*, 14, 20, (2021), 6611 <https://doi.org/10.3390/en14206611>
- [4] Huangang Shi, Chao Su, Ran Ran, Jiafeng Cao, Zongping Shao, Electrolyte materials for intermediate-temperature solid oxide fuel cells, *Progress in Natural Science: Materials International*, 30, 6, (2020), 764-774 <https://doi.org/10.1016/j.pnsc.2020.09.003>
- [5] Beom-Kyeong Park, Scott A. Barnett, Boosting solid oxide fuel cell performance via electrolyte thickness reduction and cathode infiltration, *Journal of Materials Chemistry A*, 8, 23, (2020), 11626-11631 <https://doi.org/10.1039/D0TA04280C>
- [6] Michał Mosiałek, Małgorzata Zimowska, Dmitry Kharytonau, Anna Komenda, Miłosz Górski, Marcel Krzan, Improvement of La_{0.8}Sr_{0.2}MnO_{3-δ} Cathode Material for Solid Oxide Fuel Cells by Addition of YFe_{0.5}Co_{0.5}O₃, *Materials*, 15, 642, (2022), 1-14 <https://doi.org/10.3390/ma15020642>
- [7] Jun Ho Kim, Jeong Woo Yun, Sulfur Tolerance Effects on Sr_{0.92}Y_{0.08}Ti_{0.5}Fe_{0.5}O_{3-δ} as an Alternative Anode in Solid Oxide Fuel Cells, *Journal of Electrochemical Science and Technology*, 9, 2, (2018), 133-140 <https://doi.org/10.5229/JECST.2018.9.2.133>
- [8] Andrei I. Klyndyuk, Ekaterina A. Chizhova, Dzmitry S. Kharytonau, Dmitry A. Medvedev, Layered oxygen-deficient double perovskites as promising cathode materials for solid oxide fuel cells, *Materials*, 15, 1, (2021), 141 <https://doi.org/10.3390/ma15010141>
- [9] Renato Pelosato, Giulio Cordaro, Davide Stucchi, Cinzia Cristiani, Giovanni Dotelli, Cobalt based layered perovskites as cathode material for intermediate temperature Solid Oxide Fuel Cells: A brief review, *Journal of Power Sources*, 298, (2015), 46-67 <https://doi.org/10.1016/j.jpowsour.2015.08.034>
- [10] Wei Xia, Xianglin Liu, Fangjun Jin, Xuelin Jia, Yu Shen, Jinhua Li, Evaluation of calcium codoping in double perovskite PrBaCo₂O_{5+δ} as cathode material for IT-SOFCs, *Electrochimica Acta*, 364, 137274, (2020), 1-11 <https://doi.org/10.1016/j.electacta.2020.137274>
- [11] Quan Yang, Dong Tian, Rui Liu, Haodong Wu, Yonghong Chen, Yanzhi Ding, Xiaoyong Lu, Bin Lin, Exploiting rare-earth-abundant layered perovskite cathodes of LnBa_{0.5}Sr_{0.5}Co_{1.5}Fe_{0.5}O_{5+δ} (Ln= La and Nd) for SOFCs, *International Journal of Hydrogen Energy*, 46, 7, (2021), 5630-5641 <https://doi.org/10.1016/j.ijhydene.2020.11.031>
- [12] Hailei Zhao, Yu Zheng, Chunyang Yang, Yongna Shen, Zhihong Du, Konrad Swierczek, Electrochemical performance of Pr_{1-x}Y_xBaCo₂O_{5+δ} layered perovskites as cathode materials for intermediate-temperature solid oxide fuel cells, *International Journal of Hydrogen Energy*, 38, 36, (2013), 16365-16372 <https://doi.org/10.1016/j.ijhydene.2013.10.003>
- [13] Li-Na Xia, Zhi-Ping He, X. W. Huang, Yan Yu, Synthesis and properties of SmBaCo_{2-x}Ni_xO_{5+δ} perovskite oxide for IT-SOFC cathodes, *Ceramics International*, 42, 1, (2016), 1272-1280 <https://doi.org/10.1016/j.ceramint.2015.09.062>
- [14] Xiubing Huang, Jie Feng, Hassan R. S. Abdellatif, Jing Zou, Guan Zhang, Chengsheng Ni, Electrochemical evaluation of double perovskite PrBaCo_{2-x}Mn_xO_{5+δ} (x= 0, 0.5, 1) as promising cathodes for IT-SOFCs, *International Journal of Hydrogen Energy*, 43, 18, (2018), 8962-8971 <https://doi.org/10.1016/j.ijhydene.2018.03.163>
- [15] Matthew West, Arumugam Manthiram, Layered LnBa_{1-x}Sr_xCoCuO_{5+δ} (Ln= Nd and Gd) perovskite cathodes for intermediate temperature solid oxide fuel cells, *International Journal of Hydrogen Energy*, 38, 8, (2013), 3364-3372 <https://doi.org/10.1016/j.ijhydene.2012.12.133>
- [16] Sangwook Joo, Junyoung Kim, Jeeyoung Shin, Tak-Hyoung Lim, Guntae Kim, Investigation of a layered perovskite for IT-SOFC cathodes: B-site Fe-doped YBa_{0.5}Sr_{0.5}Co_{2-x}Fe_xO_{5+δ}, *Journal of The Electrochemical Society*, 163, 14, (2016), F1489-F1495 <https://doi.org/10.1149/2.0371614jes>
- [17] Adi Subardi, Ching-Cheng Chen, Meng-Hsien Cheng, Wen-Ku Chang, Yen-Pei Fu, Electrical, thermal and electrochemical properties of SmBa_{1-x}Sr_xCo₂O_{5+δ} cathode materials for intermediate-temperature solid oxide fuel cells, *Electrochimica Acta*, 204, (2016), 118-127 <https://doi.org/10.1016/j.electacta.2016.04.069>

- [18] Chihiro Kuroda, Kun Zheng, Konrad Świerczek, Characterization of novel $\text{GdBa}_{0.5}\text{Sr}_{0.5}\text{Co}_{2-x}\text{Fe}_x\text{O}_{5+\delta}$ perovskites for application in IT-SOFC cells, *International Journal of Hydrogen Energy*, 38, 2, (2013), 1027–1038 <https://doi.org/10.1016/j.ijhydene.2012.10.085>
- [19] Fuchang Meng, Tian Xia, Jingping Wang, Zhan Shi, Jie Lian, Hui Zhao, Jean-Marc Bassat, Jean-Claude Grenier, Evaluation of layered perovskites $\text{YBa}_{1-x}\text{Sr}_x\text{Co}_2\text{O}_{5+\delta}$ as cathodes for intermediate-temperature solid oxide fuel cells, *International Journal of Hydrogen Energy*, 39, 9, (2014), 4531–4543 <https://doi.org/10.1016/j.ijhydene.2014.01.008>
- [20] Kun Zheng, Konrad Świerczek, Joanna Bratek, Alicja Klimkiewicz, Cation-ordered perovskite-type anode and cathode materials for solid oxide fuel cells, *Solid State Ionics*, 262, (2014), 354–358 <https://doi.org/10.1016/j.ssi.2013.11.009>
- [21] Rong-Tsu Wang, Horng-Yi Chang, Jung-Chang Wang, An Overview on the Novel Core-Shell Electrodes for Solid Oxide Fuel Cell (SOFC) Using Polymeric Methodology, *Polymers*, 13, 16, (2021), 2774 <https://doi.org/10.3390/polym13162774>
- [22] Adi Subardi, Meng-Hsien Cheng, Yen-Pei Fu, Chemical bulk diffusion and electrochemical properties of $\text{SmBa}_{0.6}\text{Sr}_{0.4}\text{Co}_2\text{O}_{5+\delta}$ cathode for intermediate solid oxide fuel cells, *International Journal of Hydrogen Energy*, 39, 35, (2014), 20783–20790 <https://doi.org/10.1016/j.ijhydene.2014.06.134>
- [23] Lifang Nie, Mingfei Liu, Yujun Zhang, Meilin Liu, $\text{La}_{0.6}\text{Sr}_{0.4}\text{Co}_{0.2}\text{Fe}_{0.8}\text{O}_{3-\delta}$ cathodes infiltrated with samarium-doped cerium oxide for solid oxide fuel cells, *Journal of Power Sources*, 195, 15, (2010), 4704–4708 <https://doi.org/10.1016/j.jpowsour.2010.02.049>
- [24] Adi Subardi, Yen-Pei Fu, Electrochemical and thermal properties of $\text{SmBa}_{0.5}\text{Sr}_{0.5}\text{Co}_2\text{O}_{5+\delta}$ cathode impregnated with $\text{Ce}_{0.8}\text{Sm}_{0.2}\text{O}_{1.9}$ nanoparticles for intermediate-temperature solid oxide fuel cells, *International Journal of Hydrogen Energy*, 42, 38, (2017), 24338–24346 <https://doi.org/10.1016/j.ijhydene.2017.08.010>
- [25] Jinhua Piao, Kening Sun, Naiqing Zhang, Xinbing Chen, Shen Xu, Derui Zhou, Preparation and characterization of $\text{Pr}_{1-x}\text{Sr}_x\text{FeO}_3$ cathode material for intermediate temperature solid oxide fuel cells, *Journal of Power Sources*, 172, 2, (2007), 633–640 <https://doi.org/10.1016/j.jpowsour.2007.05.023>
- [26] Yen-Pei Fu, Jie Ouyang, Chien-Hung Li, Shao-Hua Hu, Chemical bulk diffusion coefficient of $\text{Sm}_{0.5}\text{Sr}_{0.5}\text{CoO}_{3-\delta}$ cathode for solid oxide fuel cells, *Journal of Power Sources*, 240, (2013), 168–177 <https://doi.org/10.1016/j.jpowsour.2013.03.138>
- [27] Shiquan Lü, Xiangwei Meng, Yuan Ji, Chengwei Fu, Cuicui Sun, Hongyuan Zhao, Electrochemical performances of $\text{NdBa}_{0.5}\text{Sr}_{0.5}\text{Co}_2\text{O}_{5+x}$ as potential cathode material for intermediate-temperature solid oxide fuel cells, *Journal of Power Sources*, 195, 24, (2010), 8094–8096 <https://doi.org/10.1016/j.jpowsour.2010.06.061>
- [28] Abhishek Jaiswal, Eric D. Wachsman, Bismuth-ruthenate-based cathodes for IT-SOFCs, *Journal of the Electrochemical Society*, 152, 4, (2005), A787–A790 <https://doi.org/10.1149/1.1866093>
- [29] Jiyou Kim, Won-yong Seo, Jeeyoung Shin, Meilin Liu, Guntae Kim, Composite cathodes composed of $\text{NdBa}_{0.5}\text{Sr}_{0.5}\text{Co}_2\text{O}_{5+\delta}$ and $\text{Ce}_{0.9}\text{Gd}_{0.1}\text{O}_{1.95}$ for intermediate-temperature solid oxide fuel cells, *Journal of Materials Chemistry A*, 1, 3, (2013), 515–519 <https://doi.org/10.1039/C2TA00025C>
- [30] Arumugam Manthiram, Jung-Hyun Kim, Young Nam Kim, Ki-Tae Lee, Crystal chemistry and properties of mixed ionic-electronic conductors, *Journal of Electroceramics*, 27, 2, (2011), 93–107 <https://doi.org/10.1007/s10832-011-9635-x>
- [31] Abdullah Abdul Samat, Abdul Azim Jais, Mahendra Rao Somalu, Nafisah Osman, Andanastuti Muchtar, Kean Long Lim, Electrical and electrochemical characteristics of $\text{La}_{0.6}\text{Sr}_{0.4}\text{CoO}_{3-\delta}$ cathode materials synthesized by a modified citrate-EDTA sol-gel method assisted with activated carbon for proton-conducting solid oxide fuel cell application, *Journal of Sol-Gel Science and Technology*, 86, 3, (2018), 617–630 <https://doi.org/10.1007/s10971-018-4675-1>
- [32] Adi Subardi, Kun-Yu Liao, Yen-Pei Fu, Oxygen transport, thermal and electrochemical properties of $\text{NdBa}_{0.5}\text{Sr}_{0.5}\text{Co}_2\text{O}_{5+\delta}$ cathode for SOFCs, *Journal of the European Ceramic Society*, 39, 1, (2019), 30–40 <https://doi.org/10.1016/j.jeurceramsoc.2018.01.022>
- [33] Yinkai Lei, Tian-Le Cheng, You-Hai Wen, Phase field modeling of microstructure evolution and concomitant effective conductivity change in solid oxide fuel cell electrodes, *Journal of Power Sources*, 345, (2017), 275–289 <https://doi.org/10.1016/j.jpowsour.2017.02.007>
- [34] Atef Zekri, Martin Knipper, Jürgen Parisi, Thorsten Plaggenborg, Microstructure degradation of Ni/CGO anodes for solid oxide fuel cells after long operation time using 3D reconstructions by FIB tomography, *Physical Chemistry Chemical Physics*, 19, 21, (2017), 13767–13777 <https://doi.org/10.1039/C7CP02186K>
- [35] Adi Subardi, Kun-Yu Liao, Yen-Pei Fu, Oxygen permeation, thermal expansion behavior and electrochemical properties of $\text{LaBa}_{0.5}\text{Sr}_{0.5}\text{Co}_2\text{O}_{5+\delta}$ cathode for SOFCs, *RSC Advances*, 7, 24, (2017), 14487–14495 <https://doi.org/10.1039/C7RA00125H>